NASA Technical Memorandum 104371
AIAA-91-2495

Development of Braided Rope Seals for Hypersonic Engine Applications Part II: Flow Modeling

Rajakkannu Mutharasan
Drexel University
Philadelphia, Pennsylvania

Bruce M. Steinetz
Lewis Research Center
Cleveland, Ohio

and

Xiaoming Tao and Frank Ko
Drexel University
Philadelphia, Pennsylvania

Prepared for the
27th Joint Propulsion Conference
sponsored by the AIAA, SAE, and ASME
Sacramento, California, June 24-26, 1991

Development of Braided Rope Seals for Hypersonic Engine Applications Part II: Flow Modeling

By

Rajakkannu Mutharasan
Department of Chemical Engineering
Drexel University
Philadelphia, PA 19104

Bruce M. Steinetz
NASA Lewis Research Center
Cleveland, OH 44135

Xiaoming Tao and Frank Ko
Fibrous Materials Research Center
Drexel University
Philadelphia, PA 19104

ABSTRACT

Two models based on the Kozeny-Carmen equation have been developed to analyze the fluid flow through a new class of braided rope seals under development for advanced hypersonic engines. A hybrid seal geometry consisting of a braided sleeve and a substantial amount of longitudinal fibers with high packing density was selected for development based on its low leakage rates. The models developed allow prediction of the gas leakage rate as a function of fiber diameter, fiber packing density, gas properties, and pressure drop across the seal. The first model treats the seal as a homogeneous fiber bed. The second model divides the seal into two homogeneous fiber beds identified as the core and the sheath of the seal. Flow resistances of each of the main seal elements are combined to find a total flow resistance using the electrical resistance analog. Comparisons are made between measured leakage rates collected for seal structures covering a wide range of braid architectures and model predictions. It has been found that within the experimental range, the second model provides a satisfactory prediction of the flow for many of the cases examined. Areas where future model refinements are required have been identified.

NOMENCLATURE

A_c	=	Cross sectional area of seal
A_y	=	Yarn cross-sectional area
D_f	=	Fiber diameter
g_c	=	Gravitational constant
$\dot{M}$	=	Mass flow rate of gas
M_w	=	Molecular weight of gas
N_c	=	Number of core yarns
N_s	=	Number of sheath yarns
P_o	=	Pressure downstream of seal
P_i	=	Pressure upstream of seal
R_g	=	Universal gas constant
T	=	Absolute temperature
t, t_1, t_2	=	Seal dimensions (see Figure 4)
u	=	Superficial gas velocity
y_o	=	Half the clearance between the seal and its housing
ε	=	Porosity
ϕ	=	Shape factor, defined in Equation (4)
θ	=	Braid angle
ρ_f	=	Fiber density
μ	=	Gas viscosity
ρ	=	Gas density

Subscripts:

c	Core
e	Edge
sl	Seal
s	Sheath
1,2...7	Flow paths (see Figure 4)

INTRODUCTION

In the first part of this series of papers [1] , the relationship between fiber architecture and flow resistance was examined by an experimental study. A hybrid geometry consisting of a braiding sleeve and a substantial amount of longitudinal fibers was recommended. Critical design parameters were identified: fiber diameter, yarn bundle size and fiber packing density. The purpose of this paper is to provide means of analyzing the gas flow through a braided seal and determining quantitatively the relationship between the gas leakage rate and the pore structure of the seal.

THEORETICAL

Definition of Flow Path

As shown in Figure 1, the flow across a seal system can be divided into two categories: (1) flow through the seal and (2) flow around seal. The flow in the first path is related to the packing architecture of the seal itself and the flow via the second path is dependent on the surface properties of the seal and housing.

1. Flow through seal

Based on data from a large amount of experimental data obtained using a variety of packing materials, both spherical and granular in shape, Ergun [2] derived the following equation:

$$\frac{-(P_o - P_i)g_c}{\rho u^2}\frac{(\phi D)}{t}\frac{\varepsilon^3}{1-\varepsilon} = \frac{150(1-\varepsilon)}{(\phi D)\rho u/\mu} + 1.75 \qquad (1)$$

where P denotes pressure, subscripts i the inlet and o the outlet, u the average velocity of the gas across the flow area, μ the viscosity of the gas, g_c the gravitational constant, t the thickness of the bed and ε is the packed bed porosity. In the above equation, if the Reynolds number $N_{Re} = (\phi D)\rho u/\mu(1-\varepsilon)$, is small, then the constant 1.75 on the right side of the equation can be ignored. In the case of engine seal, the flow is expected to be laminar as the gas leakage rate and the fiber diameter are small. This implies that viscous term dominates in the above equation and the inertial term is negligible. Under such a condition, the pressure drop is proportional to flow velocity u.

In earlier studies the tortuous pore structure of the bed was modeled as a solid bed consisting an assembly of capillaries with circular cross section [3]. The capillary model focused on the spaces or the pores in the porous solid. The best known equation proposed based on this approach is the Kozeny-Carman equation [4], which includes permeability coefficient as a function of porosity. One form of this equation is given below as:

$$u = \frac{-(P_o - P_i)g_c}{150\frac{\mu t}{(\phi D)^2}\frac{(1-\varepsilon)^2}{\varepsilon^3}} \qquad (2)$$

The shape factor, ϕ is defined as :

$$\phi = \frac{\text{area of sphere equivalent to particle volume}}{\text{actual surface area of particle}}$$

The shape factor, ϕ is unity for a sphere and 0.87 for a cylinder with its diameter equal to its length. The equivalent diameter of a particle is defined as the diameter of a sphere having the same volume as the particle. For a fiber with a diameter D_f and length L, the equivalent diameter is

$$D = (1.5D_f^2 L)^{1/3} \qquad (3)$$

and the shape factor is

$$\phi = (1.5)^{2/3}\frac{(L/D_f)^{2/3}}{L/D_f + 0.5} \qquad (4)$$

Hence, (ϕD) can be expressed as

$$(\phi D) = 1.5\, D_f \frac{L/D_f}{L/D_f + 0.5} \qquad (5)$$

If the ratio L/D_f is very large the term (ϕD) will approach the value of $1.5D_f$. If direction of flow is across the axis of fiber, a situation that occurs in a seal containing substantial amount of longitudinal fibers, the length scale, L in the above equation should be expected to be of the same order of magnitude as the diameter of the fiber. The parameter (ϕD) can be thought of as characteristic dimension intrinsic to flow through the fibrous seal.

The Kozeny-Carman equation predicts successfully the pressure drop in packed beds with porosity ranging from 0.3 to 0.6. For porous media with higher porosity such as most fiber beds and textile fabrics, a number of authors [for example see ref. 5] have shown that predicted pressure drop is much greater than experimentally measured values. In the current application, for determining leakage rate of a gas through a seal having low porosity, Kozeny-Carman equation is a good starting point. Taking cross sectional area for gas flow as A_C and the seal length as L, Equation (2) after multiplied by $A_C\rho/L$ can then be rearranged to express gas leakage rate per unit length of seal as:

$$\frac{\dot{M}}{L} = \frac{-(P_o^2 - P_i^2)}{300\frac{\mu R_g T}{M_w g_c}\frac{tL}{A_c}\frac{(1-\varepsilon)^2}{\varepsilon^3(\phi D)^2}} \qquad (6)$$

where ideal behavior of gas is assumed. The density of gas, ρ is based on an average value evaluated at the two end-point pressures. That is,

$$\rho = \frac{(P_o + P_i)M_w}{2R_g T} \qquad (7)$$

where R_g is the gas constant, M_w is molecular weight of the gas, T is the absolute temperature.

2. Flow around seal

Edge flow can be treated as a flow between parallel non-porous surfaces separated by a small gap. Assuming that the gap between the surfaces can be considered constant equal to $2y_0$, one can relate the pressure difference across the seal to the gas leakage velocity as [6]

$$P_o - P_i = \frac{3\mu u t}{g_c y_o^2} \qquad (8)$$

Rearranging the above in the form of Equation (6) gives

$$\frac{\dot{M}}{L} = \frac{-(P_o^2 - P_i^2)}{\frac{3\mu R_g T}{M_w g_c}\frac{t}{y_o^3}} \qquad (9)$$

where ideal gas behavior is assumed and average gas density is used.

3. Flow resistance

Examination of Equation (6) for flow though the seal and Equation (9) for flow around the seal suggests the definition of flow resistance R as:

$$R = \frac{-(P_o^2 - P_i^2)}{\frac{\dot{M}}{L}} \qquad (10)$$

The flow resistance, R is a function of properties of both fluid and seal architecture and, for this analysis, is assumed to be independent of the pressure difference across it and any compressive pressure the seal may be subjected to.

Flow Modeling

In a previous paper [1], critical design parameters such as fiber packing density and fiber bundle size were identified through a combination of theoretical and experimental studies. It was shown that a hybrid geometry consisting of a braiding sleeve and a substantial number of longitudinal fibers can be employed as the fundamental structure for high temperature flexible fibrous seals. Since the seal consists of both braids in the sheath and longitudinal fibers in the core, one expects different porosity values to be applicable in the two regions. In this investigation, two models are proposed to quantitatively evaluate the flow resistances. In the first, we will consider the entire seal to have one constant porosity value, while in the second model we will treat the core and the sheath to have two separate porosity values.

1. Model I

In the first model, the seal is assumed to be a homogeneous fiber bed having a uniform constant porosity regardless of the core and sheath structures. Thus, only one value of porosity is used to calculate the flow resistance. As shown in Figure 2, the gas leakage rate can be expressed as the sum of the leakages through the seal and around the seal and is given by

$$\frac{\dot{M}}{L}=\frac{\dot{M}_e}{L}+\frac{\dot{M}_{sl}}{L}=\frac{(P_i^2-P_o^2)}{R} \quad (11)$$

where subscripts, sl and e refer to the seal and edge respectively. The individual leakages are given by

$$\frac{\dot{M}_e}{L}=\frac{(P_i^2-P_o^2)}{R_e} \quad (12)$$

$$\frac{\dot{M}_{sl}}{L}=\frac{(P_i^2-P_o^2)}{R_{sl}} \quad (13)$$

The flow resistances of encountered in the flow path through the seal is determined from Equation (6) and is given as:

$$R_{sl}=300\frac{\mu R_g T t L (1-\varepsilon)^2}{M_w g_c A_C \varepsilon^3 (\phi D)^2} \quad (14)$$

The edge flow consists of two parallel paths as shown in Figure 2 and the flow resistance of each of these two paths may be summed in parallel as

$$R_e=\frac{R_{e1}R_{e2}}{R_{e1}+R_{e2}} \quad (15)$$

with

$$R_{e1}=9\frac{\mu R_g T}{M_w g_c}\frac{t}{y_o^3} \quad \text{and} \quad R_{e2}=3\frac{\mu R_g T}{M_w g_c}\frac{t}{y_o^3}$$

where R_{e1} is three times R_{e2} because of the longer path length, see Figure 2. Since the edge flow and flow through the seal occur in parallel, the overall flow resistance of the seal system is therefore given by

$$R=\frac{R_e R_{sl}}{R_e+R_{sl}} \quad (16)$$

2. Model II

The second model, illustrated in Figure 3, deals with a composite seal in which the sheath and core are allowed to have independent porosity values. The seal has a sheath and a core with porosities ε_s and ε_c, respectively. Flow resistances along the various flow paths illustrated in Figure 4, are given as:

$$R_1=9K\frac{t}{y_o^3} \quad (17)$$

$$R_2=R_6=300\,K\frac{t}{t_2}\frac{(1-\varepsilon_s)^2}{\varepsilon_s^3(\phi D)^2} \quad (18)$$

$$R_3=R_5=300\,K\frac{t_2}{t}\frac{(1-\varepsilon_s)^2}{\varepsilon_s^3(\phi D)^2} \quad (19)$$

$$R_4=300\,K\frac{(1-\varepsilon_c)^2}{\varepsilon_c^3(\phi D)^2} \quad (20)$$

$$R_{345}=R_3+R_4+R_5 \quad (21)$$

$$R_7=3K\frac{t}{y_o^3} \quad (22)$$

where $K=\frac{\mu R_g T}{M_w g_c}$. The flow resistance of the seal can be determined by summing the flow resistances in parallel, given as:

$$\frac{1}{R_s}=\frac{1}{R_2}+\frac{1}{R_{345}}+\frac{1}{R_6} \quad (23)$$

Flow resistance of edge flow is:

$$R_e=\frac{R_1 R_7}{R_1+R_7} \quad (24)$$

The total flow resistance of the seal system is then given by:

$$R=\frac{R_e R_s}{R_e+R_s} \quad (25)$$

Calculation Basis

One of the important parameters in determining flow resistance through the seal is the characteristic dimension, D. Considering that the bulk of the seal is made up of longitudinal fibers and that the number of fiber-fiber interfaces is significantly larger than the number of yarn-yarn interfaces, the

characteristic dimension was taken as the fiber diameter, D_f. The characteristic dimension, (ϕD), takes on values between $1.5D_f$ and $0.75D_f$ when the ratio L/D_f is taken to be large or 0.5, respectively. The latter value gives better fit with experimental data under a variety of situations investigated. Therefore, all calculations presented in this paper are based on the shape factor value of 0.75. It should be noted that the better fit of experimental data with $(\phi D)=0.75D_f$ is indicative of the fact that the dominant gas flow path is across the fiber bundle rather than along the fiber bundle.

Another characteristic dimension is the distance, y_o in calculating seal edge leakage. In the present calculation, the clearance was assumed to be proportional to fiber diameter. Specifically y_o is assumed to be 0.1 (ϕD).

The cross section area of a yarn A_y (in^2) can be determined from its denier (grams per 9000 meters of fiber) and fiber density ρ (g/cm^3) as follows:

$$A_y = \frac{\text{yarn denier}}{5.8\text{x}10^6 \rho_f} \qquad (26)$$

The following are the parameters used for calculation of various flow properties.

$\rho_f = 2.54\ g/cm^3$	denier= 812 g / 9000 m
$R_g = 1.545 \times 10^3$ lb-ft/^{0}R	T = 528 ^{0}R
D_f = 10 microns	$g_c = 32.1\ lb_m ft/lb_f\ sec^2$
M_w(air) = 29 lb_m/lb mole	M_w(He) = 4 lb_m/lb mole
$(\phi D) = 0.75\ D_f$	$y_o = 0.1\ (\phi D)$
μ of air = 0.0175 cP	μ of He = 0.019 cP

EXPERIMENTAL

Braided Seals Specimens

Eight seal specimens were made using 812 denier E-glass fibers (Owens Corning Glass, Granville, Ohio). The specimens were labeled A1 through H1 and their architectural parameters, braiding angle, number of longitudinal yarns and number of braiding yarns, are summarized in Table 1. Specimens G1 and H1 have the highest number of longitudinal yarns while A1, B1 and C1 have the lowest longitudinal yarns.

Flow Measurement

The experimental details of the flow measurement were described in an earlier paper by the authors [1]. Seal specimens one foot in length were mounted in a specially developed test fixture and were leak tested under room temperature at various inlet pressure conditions in the range of 5 to 60 psig. The pressure upstream of the seal was varied and the resulting leakage of gas (either air or helium) was measured. Lateral preloads were applied uniformly to the back of the seal with an inflatable rubber diaphragm at either 80 or 130 psig. The flow resistance of the seal was computed from the ratio of the difference of the squares of absolute pressures over the mass leakage rate.

Porosity measurement

1. Sample preparation

An ultra-low viscosity embedding media (purchased from Polysciences Inc., Warrington, PA) was used as a rigidizing medium. The components were combined gravimetrically into an oven-dry beaker with a magnetic stirrer for 1-2 minutes at low speed. The components used are:

Epoxy resin	VCD (Vinyl Cyclohexane Dioxide)	0.5 part
Hardener	N- Octenyl Succinic Anhydride	1.0 part
Modifier	1,4-Butanediol Diglycidyl Ether	0.075 part
Catalyst	DMAE(Dimethylaminoethanol)	1.0% Vol.

After a graded series of alcohol changes (approximately 5 minutes each) and several 10-minute change of 100% alcohol, the specimen was infiltrated for 10 minutes in a 1:1 resin/100% alcohol mix. Final infiltration consisted of 100% embedding media for 15 minutes. Polymerization was accomplished at 70^{0}C for 12 hours. The specimen then was cut by a diamond saw and put into polyethylene moulding capsules containing Lecoset 7000 cold curing resin. Curing took place at room temperature for about 10 minutes. After demoulding, the specimen surface was polished and

scanning electron micrographs were taken to determine the dimension of the seal cross section and packing geometry of fibers.

2. Determination of porosity

Porosity of the seal for calculating flow resistances described earlier was obtained from the geometry of fiber layout and is given by:

$$\varepsilon = 1 - \frac{A_y(N_c + N_s/\cos\theta)}{t^2} \qquad (27)$$

where N_c and N_s are the number of core and sheath yarns and t^2 is the cross sectional area of the installed seal and θ is the sheath braiding angle. Note that the seal is treated as a homogeneous fiber bed having a single average porosity value for Model I.

The porosity of the core and sheath sections of the specimens for Model II were determined from the following two equations:

$$\varepsilon_c = 1 - \frac{A_y N_c}{t_1^2} \qquad (28)$$

$$\varepsilon_s = 1 - \frac{A_y N_s/\cos\theta}{t^2 - t_1^2} \qquad (29)$$

where t and t_1 are the overall width of the installed seal, and the width of the core region, respectively (see Figure 4).

RESULTS AND DISCUSSION

Pressure Drop Correlations

In Figure 5, typical air leakage rates measured are plotted as a function of difference of the squares of the pressure across the seal for specimens F1 and G1 at preload pressures of 80 and 130 psig. The linear relationship between the two variables is indicative of the validity of the pressure dependency presented earlier in Equation (10). Although only two sample results are shown in Figure 5, all eight specimens examined in this investigation showed excellent correlation with correlation coefficient lying in the range of 0.97 to 1.00. The slope of the line in Figure 5 is equal to the inverse of flow resistance, 1/R.

Flow Resistances for Different Gases

Because of the many environments the seals are expected to operate in, it is important to be able to predict the resistance to flow for various potential coolant or leakage gases. Shown in Figure 6 is the measured resistances of helium plotted against the resistance of air for a wide range of seal architectures (specimens A1 to H1), pressure drop conditions (between 5 to 60 psig), and preload conditions (80 psig and 130 psig) investigated. If the seal's pore structure is constant, flow resistance is directly proportional to viscosity and inversely proportional to molecular weight of the flowing gas (see for example Equation 6). Hence, when we compare the flow resistance of helium to that of air in Figure 6, we expect the slope of the straight line to be

$$\text{SLOPE} = \frac{(\mu/M_w)_{\text{Helium}}}{(\mu/M_w)_{\text{Air}}} \qquad (30)$$

The straight line indicated in Figure 6 is the theoretical line with a slope of 7.87 obtained using Equation (30). Data in Figure 6 show good agreement between the measured and the theoretical predictions. It is important to note that for the same seal architecture and the same pressure drop across the seal the helium leakage rate is only one-eighth of the air leakage rate.

Comparison of Measured and Predicted Leakage Rates

The measured and predicted leakage rates for two widely different seal architectures are shown in Figures 7 and 8. Key braiding and geometry parameters of these two seal structures denoted Al and Gl are listed in Table 1. Comparing the overall leakage rates between specimen Al and Gl one finds that the leakage rates for Gl are considerably less than Al. Specimen Gl meets the tentative leakage limit of 0.004 lb/sec/ft [7] for air pressure differentials up to ~51 psi with a preload of 80 psig. Specimen Al meets the leakage limit for pressure differentials only up to 30 psi. Measured and predicted leakage rates for specimen Al are shown in Figure 7 for applied pressure differentials up to 60 psi for both air and helium test gases. Also shown in the figure are the effects of lateral preload on seal leakage. Lateral preloads of 80 and 130 psig were applied to the back of seal with a diaphragm

compressing the seal against the adjacent sidewall [see ref. 1].

In general the more detailed model (Model II) that treats the seal as a composite sheath-core structure provides a conservative leakage estimate that agrees reasonably well with the measured data over the full pressure range for both air and helium test gases.

Measured and predicted leakage rates for the lower permeability seal Gl are shown in Figure 8 for air and helium and for the two preload pressures mentioned above.

For this lower leakage seal structure both models predict higher leakage rates than the measured values. Agreement between the measured and predicted is better for the lighter 80 psig preload than for the 130 psig preload.

In examining Figures 7(a) and 8(a), the versatility of Model II in predicting actual leakage rates is demonstrated. At a pressure differential of 40 psi the discrepancy between the measured and predicted leakage rates were only between 20 to 30 percent even though the overall leakage rates differed by a factor of 2.50.

In all the cases, the fiber diameter was used as the basis of calculation. However, if yarn diameter is used as the equivalent diameter, the prediction of the gas leakage rate is very poor as it differs from experimental observation by more than four orders of magnitude.

Potential Sources of Modeling Discrepancy

Effect of shape factor

The choice of shape factor ϕ has a considerable effect on the predicted leakage rates. For example, since in Equation (6) the term containing (ϕD) is squared, reducing it from 0.75 to 0.70 reduces the predicted leakage by 13%. Selection of the shape factor ϕ is based on experimental observations and therefore some variation between widely differing braids is expected.

Dependence of Porosity on Preload

Another potential cause of the discrepancy between the measured and predicted leakage rates is the porosity dependence on preload. As the backside preload is increased the fibers are urged closer to one another making it more difficult for the air to flow around the fibers, thus increasing the resistance to flow. Neither of the models considered in this paper account for this porosity-load dependence since it was deemed beyond the scope of the immediate study. A more detailed model that will include porosity as a function of seal preload is presently under development.

SUMMARY AND CONCLUSIONS

Two analytical models have been developed for predicting leakage rates of braided rope seals being developed for panels of advanced hypersonic engines. Both models are based on the Kozeny-Carmen relations for flow through porous media, where the characteristic size dimension is a scaled fiber diameter (e.g. 0.75 D_f) based on experimental observations. The first model treats the seal as a homogeneous fiber bed having a single average value for its porosity.

The second model treats the two-dimensional braided seal structures as a system of flow resistances analogous to a series of resistors in an electrical network. For the purposes of this model development, resistance is defined as the ratio of the difference in the squares of the upstream and downstream pressure (e.g. the flow potential) to the mass flow per unit seal length (e.g. the current). This approach allows the fundamental inhomogeneity of the seal's core and sheath to be characterized. These resistances are added as in an electrical network (e.g. resistances in series add; resistances in parallel add by their inverses) to form an equivalent seal resistance. Each of these resistances are made up of the product of four terms: the first term captures the properties of the gas (e.g. viscosity, gas constant, temperature and molecular weight); the second term is a ratio of the length-to-thickness of that piece of seal; a term containing the reciprocal of $(0.75\ D_f)^2$; and a term containing a porosity factor (e.g. $\frac{(1-\varepsilon)^2}{\varepsilon^3}$) . The porosity for the core and sheath are determined using image analyses of epoxy-fixed seal test coupons.

For modeling purposes, the sheath is divided into four regions of resistance depending upon the

sheath's being parallel or perpendicular to flow direction. The resistance of the core is modelled by its own resistance that is markedly different from those of the sheath. Surface flows between the nose of the seal and the adjacent splitter wall and between the top of the seal and the adjacent seal channel walls are also included in the model. Adding the resistances together according to their electrical analog characterizes the seal for leakage predictions.

Comparisons are made between measured leakage rates collected for seal structures covering a wide range of braid architectures, and predictions made using the two models. Room temperature leakage measurements were collected as a function of: pressure drop applied across the seal (venting to atmospheric condition); backside seal preload; and test gas (e.g. air and helium). Generally, the more detailed flow model (Model II) is preferred since it captures the significant porosity differences between the seal's core and sheath. For modest and heavy preloads (e.g. 80 and 130 psi), the second model favorably predicts the leakage flow rates for the relatively high permeability braided seal, Al.

Similar agreement between measured and predicted leakage was observed for the low permeability braided seal (Gl) sealing air with 80 psig preload. Reasonable agreement between measured and predicted leakage was observed for G1 sealing helium gas. However for the 130 psi preload, Model II over-predicted the measured air leakage by as much as 100%. Model refinements in-progress are aimed at minimizing the noted discrepancies and accounting for the effects of seal preload on seal permeability.

It is noted however, that these predictions are substantially closer to the measured values than those obtained with the unmodified, homogeneous-porous-media predictions of the Kozeny-Carmen relations. These relations underestimate seal leakage rates by more than several orders of magnitude.

Based on these findings, the following results were obtained:

1. Leakage rates predicted using Model II agree favorably to the measured leakage rates for modest preloads for a wide range of braided seal architectures. Agreement within 20-30% was observed for seal specimens Al and Gl whose overall leakage rates differed by a factor of almost 2.5

2. Theoretical predictions confirmed with experimental observations for air and helium indicate that relative resistance to leakage flow depends on the ratio of the quotients of each gas's viscosity and molecular weight.

ACKNOWLEDGEMENT

The authors wish to thank Ms. Susan Marr for making most of the specimens and carrying out the flow measurement. The financial sponsorship of this project from NASA is gratefully acknowledged.

REFERENCES

1. Ko, F., Steinetz, B.M., Mutharasan, R., "Development of Improved Hypersonic Engine Braided Rope Seals Part I: Design Concept and Experimental Observations," To be published as a NASA TM.

2. Ergun, S.: "Fluid Flow Through Packed Columns," Chemical Engineering Progress, Vol. 48, No. 2, Feb. 1952, pp.89-94.

3. White, F. M.: Viscous Fluid Flow. McGraw Hill Book Company, New York, 1974.

4. Scheidegger, A. E., "The Physics of Flow Through Porous Media," revised ed., University of Toronto Press, Toronto, 1960.

5. Van Den Brekel, L.D.M. and De Jong, E.J.: Hydrodynamics in Packed Textile Beds, Textile Research Journal, Vol.59, no. 8, Aug, 1989, pp. 433-440.

6. Bennett, C.O. and Myers, J.E: Momentum, Heat and Mass Transfer, Third edition, McGraw-Hill Book Company, New York, 1982.

7. Steinetz, B.M., DellaCorte, C. and Sirocky, P.J., "On the Development of Hypersonic Engine Seals," NASA TP-2854, 1988.

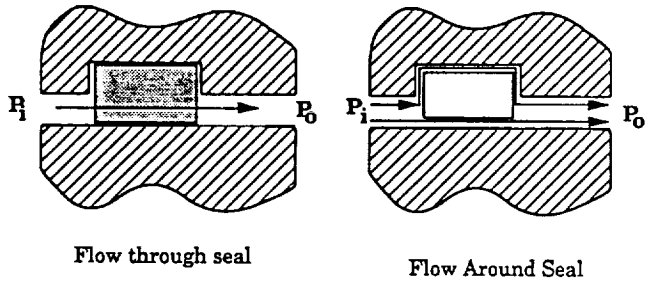

Figure 1. – Definition of seal leakage flow paths.

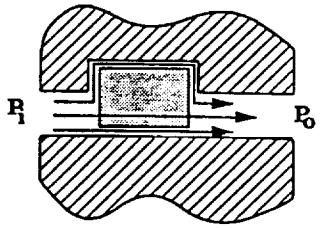

Figure 2. – Schematic diagram for flow Model I, in which the seal is treated as having an uniform porosity throughout its entire cross section.

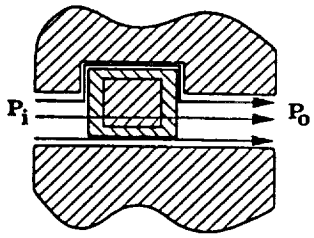

Figure 3. – Schematic diagram for the flow Model II, in which the core and sheath sections of the seal are considered to have different porosity values.

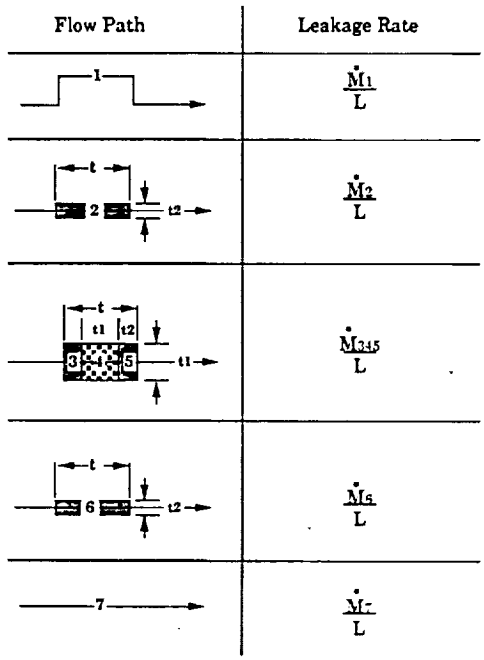

Figure 4. – Various flow paths used in calculating total flow resistance using flow Model II. The top and bottom paths given above show the flow around the seal, while the middle three paths indicate schematically the paths through the seal.

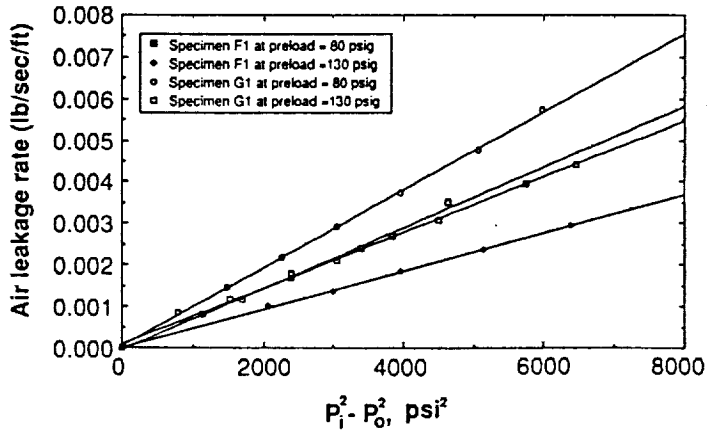

Figure 5. – Plot of air leakage rate versus difference in squares of pressure for the Seal Specimens F1 and G1 at preload pressures of 80 and 130 psig. The solid lines are a least square linear fit of experimental data.

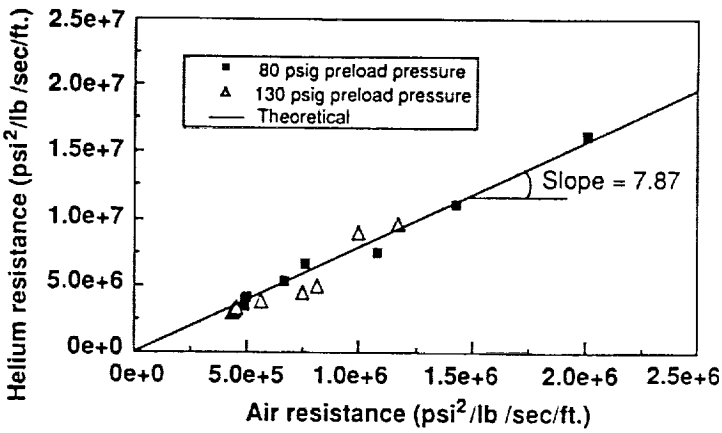

Figure 6. – Comparison of measured seal leakage flow resistances of air and helium to theoretical expectations showing excellent correlation.

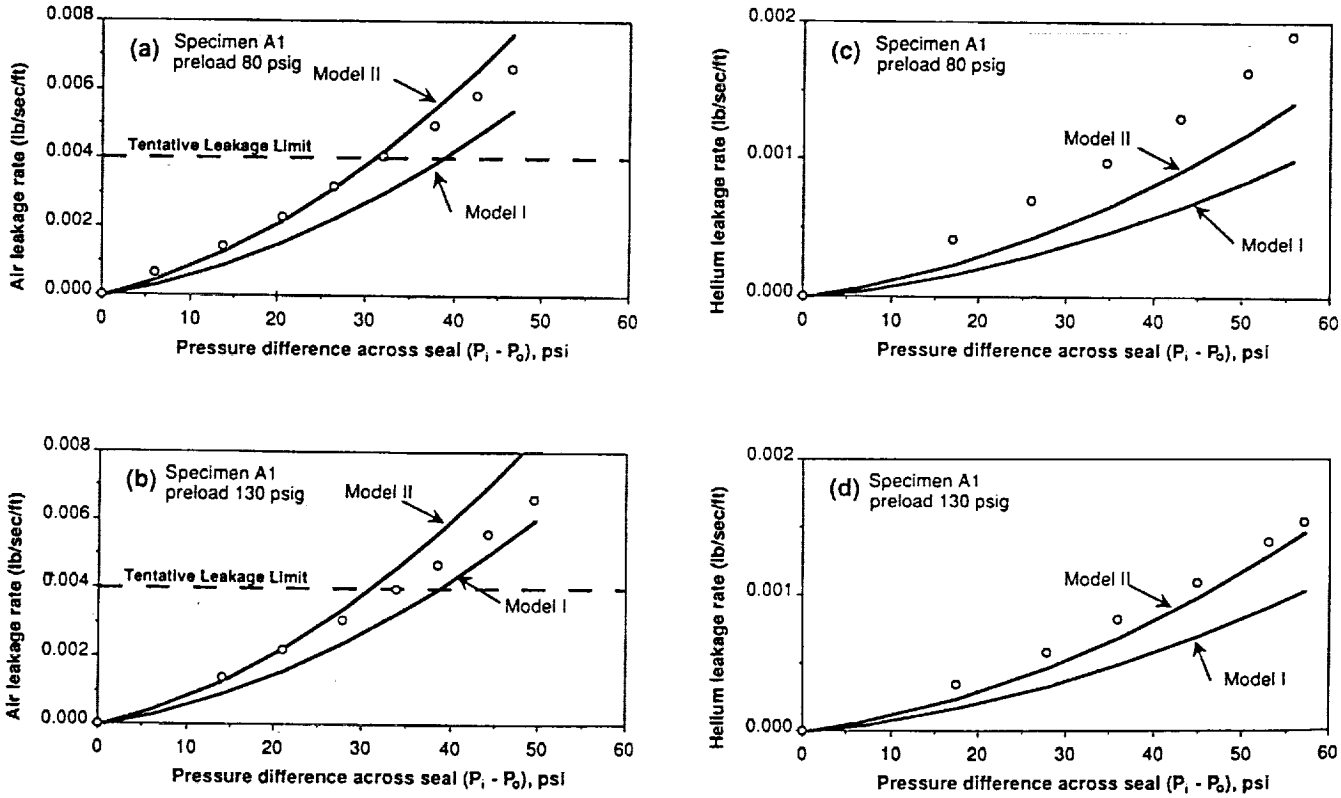

Figure 7. – Plots of gas leakage rate as a function of applied pressure differential for specimen A1: (a) air flow with preload pressure of 80 psig; (b) air flow with preload pressure of 130 psig; (c) helium flow with preload pressure of 80 psig; (d) helium flow with preload pressure of 130 psig. The solid curves are calculated from the two flow models proposed in the paper and the dots are the experimental values.

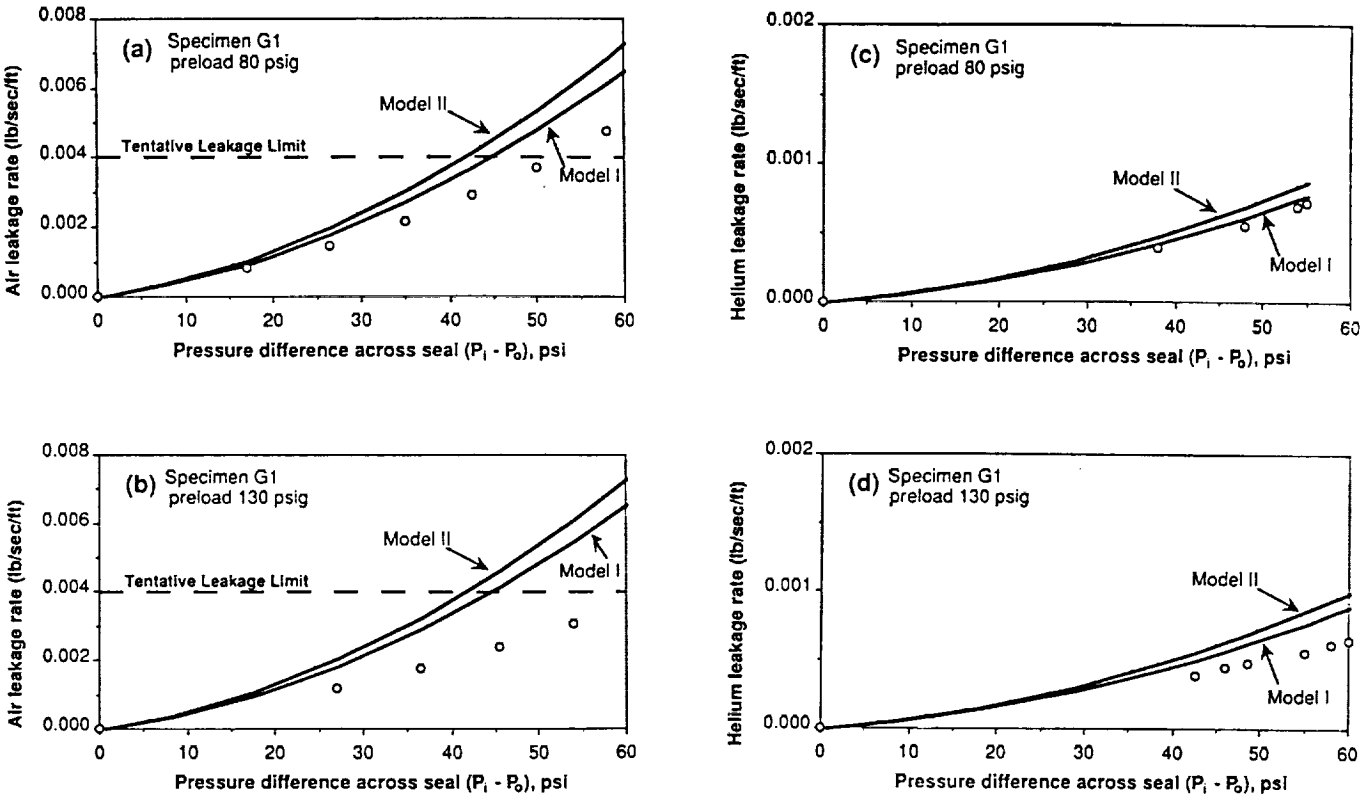

Figure 8. – Plots gas leakage rate as a function of applied pressure differential for specimen G1: (a) air flow with preload pressure of 80 psig; (b) air flow with preload pressure of 130 psig; (c) helium flow with preload pressure of 80 psig; (d) helium flow with preload pressure of 130 psig. The solid curves are calculated from the two flow models proposed in the paper and the dots are the experimental values.

Table 1: Seal Construction Details and Porosity Data

Sample No.	Braiding Angle (θ, °)	Number of Longitudinal Yarns	Number of Braider Yarn	Average Porosity	Thickness t_2* (in)	Core Porosity	Sheath Porosity
A1	45	935	1008	0.48	0.11	0.34±.04	0.54±.02
B1	30	935	1248	0.48	0.12	0.24±.06	0.56±.01
C1	10	935	1320	0.50	0.09	0.50±.03	0.50±.02
D1	45	1497	792	0.42	0.09	0.19±.05	0.58±.02
E1	30	1497	840	0.46	0.06	0.43±.03	0.49±.04
F1	10	1497	1206	0.40	0.09	0.19±.05	0.54±.02
G1	45	2042	312	0.45	0.02	0.47±.02	0.37±.16
H1	30	2042	408	0.45	0.02	0.47±.02	0.32±.18

* The accuracy of t_2 measurement was within ±0.005".

NASA
National Aeronautics and Space Administration

Report Documentation Page

1. Report No.	2. Government Accession No.	3. Recipient's Catalog No.
NASA TM -104371 AIAA-91-2495		

4. Title and Subtitle
Development of Braided Rope Seals for Hypersonic Engine Applications Part II: Flow Modeling

5. Report Date

6. Performing Organization Code

7. Author(s)
Rajakkannu Mutharasan, Bruce M. Steinetz, Xiaoming Tao, and Frank Ko

8. Performing Organization Report No.
E -6166

10. Work Unit No.
505 -63-5B

9. Performing Organization Name and Address
National Aeronautics and Space Administration
Lewis Research Center
Cleveland, Ohio 44135 - 3191

11. Contract or Grant No.

13. Type of Report and Period Covered
Technical Memorandum

12. Sponsoring Agency Name and Address
National Aeronautics and Space Administration
Washington, D.C. 20546 - 0001

14. Sponsoring Agency Code

15. Supplementary Notes
Prepared for the 27th Joint Propulsion Conference cosponsored by AIAA, SAE, and ASME, Sacramento, California, June 24-26, 1991. Rajakkannu Mutharasan, Department of Chemical Engineering, Drexel University, Philadelphia, Pennsylvania 19104. Bruce Steinetz, NASA Lewis Research Center. Xiaoming Tao and Frank Ko, Fibrous Materials Research Center, Drexel University. Responsible person, Bruce M. Steinetz, (216) 433-3302.

16. Abstract
Two models based on the Kozeny-Carmen equation have been developed to analyze the fluid flow through a new class of braided rope seals under development for advanced hypersonic engines. A hybrid seal geometry consisting of a braided sleeve and a substantial amount of longitudinal fibers with high packing density was selected for development based on its low leakage rates. The models developed allow prediction of the gas leakage rate as a function of fiber diameter, fiber packing density, gas properties, and pressure drop across the seal. The first model treats the seal as a homogeneous fiber bed. The second model divides the seal into two homogeneous fiber beds identified as the core and the sheath of the seal. Flow resistances of each of the main seal elements are combined to find a total flow resistance using the electrical resistance analog. Comparisons are made between measured leakage rates collected for seal structures covering a wide range of braid architectures and model predictions. It has been found that within the experimental range, the second model provides a satisfactory prediction of the flow for many of the cases examined. Areas where future model refinements are required have been identified.

17. Key Words (Suggested by Author(s))
Seals
Porous materials
Fluid flow
Braided rope

18. Distribution Statement
Unclassified - Unlimited
Subject Category 37

19. Security Classif. (of the report)	20. Security Classif. (of this page)	21. No. of pages	22. Price*
Unclassified	Unclassified	12	A03

NASA FORM 1626 OCT 86

*For sale by the National Technical Information Service, Springfield, Virginia 22161